RESEARCH ON HYPERSPECTRAL MONITORING OF FOXTAIL MILLET BIOMASS

QIAO, Y.[1] – LI, R.[2] – CHANG, B.[2] – ZHOU, W.[3] – TIAN, X.[4] – CHEN, L.[4] – WANG, J. J.[4*]

[1]*School of Economics and Management, Shanxi Agricultural University, Taiyuan, China*

[2]*College of Agriculture, Shanxi Agricultural University, Taigu, China*

[3]*Shanxi Institute for Functional Food, Shanxi Agricultural University, Taiyuan, China*

[4]*Center for Agricultural Genetic Resources Research, Shanxi Agricultural University/Key Laboratory of Crop Gene Resources and Germplasm Enhancement on Loess Plateau, Ministry of Agriculture/Shanxi Key Laboratory of Genetic Resources and Genetic Improvement of Minor Crops, Taiyuan, China*
(phone: +86-159-0340-1303)

[*]*Corresponding author*
e-mail: xiaoleiwangjie@163.com; phone: +86-152-3404-0919

(Received 18th Dec 2024; accepted 27th Feb 2025)

Abstract. In the context of the need for efficient agricultural monitoring under climate change, this study aimed to achieve rapid and non-destructive monitoring of foxtail millet aboveground biomass (AGB), AGB data and canopy spectral data were measured under varying sowing dates. Preprocessed using Standard Normal Variate (SNV), Multiple Scattering Correction (MSC), and First Derivative (1ST) methods. Based on this, foxtail millet AGB monitoring models were constructed using the full spectrum, characteristic wavelengths, and optimized spectral indices, and their accuracy was evaluated. The results showed that all three preprocessing methods improved the correlation between spectral reflectance and foxtail millet AGB. The best spectral index was 1ST-TB1 (451, 626, 697), which exhibited a correlation coefficient of 0.863 with foxtail millet AGB. Among the constructed models, the 1ST-PLS model based on the full spectrum exhibited higher accuracy (R^2=0.834; RMSE=1.443 t/hm^2; RPD=2.507). This study confirms the feasibility of spectral monitoring for foxtail millet AGB and provides a reference for rapid, non-destructive monitoring of foxtail millet AGB, and provide a robust framework for precision agriculture, enabling efficient foxtail millet management and yield optimization.
Keywords: *foxtail millet, remote sensing, precision agriculture, non-destructive monitoring, vegetation indices*

Introduction

Foxtail millet is one of the most important traditional food crops in China, boasting a long history of cultivation (Lv et al., 2020; Li et al., 2022b). Due to its drought tolerance, poor soil adaptability, high water use efficiency, improve soil structure and reduce soil erosion, and balanced nutrition, it remains a crucial crop in the arid and semi-arid regions of the Asia, Africa, and Eastern Europe (Lata et al., 2013; Yang et al., 2019b; Diao, 2019). Considering food security, enhancing the yield of foxtail millet is vital for ensuring regional food supply and improving farmers' incomes (Li et al., 2021c). The sowing date significantly influences the yield and quality of foxtail millet; an optimal sowing schedule aligns the growth and developmental stages of foxtail millet with favorable climatic conditions, thereby improving the utilization of water and solar heat and enhancing both yield and quality (Li et al., 2021b, 2022a). Aboveground biomass (AGB) is a critical parameter reflecting crop growth status and guiding field management, closely associated with crop yield. Research on AGB can provide a theoretical basis for high-yield cultivation of foxtail millet (Wang et al., 2023a; Zhu et al., 2023a;

http://www.aloki.hu ● ISSN 1589 1623 (Print) ● ISSN1785 0037 (Online)
DOI: http://dx.doi.org/10.15666/aeer/2302_37573771

Dong et al., 2024a). Although traditional destructive sampling methods for determining millet AGB are accurate, they are time-consuming and have a delayed response (Marshall et al., 2015; Yue et al., 2019).

Since the 1970s, remote sensing techniques have been extensively used to estimate various crop physiological parameters (Kuplich et al., 2005; Yang et al., 2019a; Jiang et al., 2022). With the advancement of high-resolution sensors and computing technology, remote sensing for monitoring crop conditions has gained increasing attention (Kang et al., 2020; Zhao et al., 2024). Specifically, hyperspectral remote sensing technology allows for the quantitative analysis of subtle changes in crop development through minor differences in spectral reflectance, offering a rapid, non-destructive method to assess foxtail millet AGB (Yan et al., 2022). Currently, spectral monitoring of crop growth parameters can be categorized into three types based on the number of wavelengths used in model construction. The first type uses the full spectrum, treating all wavelengths as variables to construct the monitoring model. For instance, Dong et al. (2019) developed a hyperspectral monitoring model for the chlorophyll content of maize leaves, which showed that models based on the full spectrum performed best (R^2=0.910, RMSE=2.071). The second type involves constructing models using characteristic wavelengths, such as the work by Xie et al. (2023) who used correlation analysis and stepwise multiple linear regression (CA+SMLR), partial least squares regression (PLS+SMLR), and the successive projection algorithm (SPA) to identify characteristic wavelengths for proline content in winter wheat. Their PLSR model demonstrated superior performance. The third type employs spectral indices to construct models. Commonly used dual-band spectral indices include the Ratio Spectral Index (RSI), Normalized Difference Spectral Index (NDSI), and Difference Spectral Index (DSI) (Zhu et al., 2023b; Zhang et al., 2023). For example, Gong et al. (2023) constructed estimation models for soybean AGB using seven different vegetation indices, finding that the model based on the Infrared Vegetation Index (IPVI) outperformed those based on other indices. Wang et al. (2023b) monitored the Leaf Area Index (LAI) and AGB of rice using multispectral images, showing strong correlations between vegetation indices and LAI and AGB, with the best indices being the Chlorophyll Red Edge Index (CIRE) and the Normalized Difference Red Edge Index (NDRE), achieving R^2 values of 0.80 and 0.76, respectively. However, when vegetation cover is high, dual-band spectral indices can saturate, failing to accurately reflect the actual condition of the vegetation. Compared to dual-band indices, three-band spectral indices can mitigate this saturation issue to some extent, providing a more comprehensive reflection of vegetation growth conditions.

Current hyperspectral studies on crop biomass predominantly focus on staple cereals (e.g., wheat, maize), while neglecting drought-adapted minor crops like foxtail millet. Existing models often rely on dual-band indices prone to saturation and lack systematic evaluation of preprocessing methods (SNV, MSC, 1ST) for spectral noise reduction. We systematically conduct a comprehensive comparison of various preprocessing techniques and different model types specifically tailored for the monitoring of AGB. This systematic approach not only addresses the long - standing neglect of foxtail millet in related research but also contributes to resolving the ambiguity in methodological choices, thereby potentially advancing the field of crop biomass monitoring with respect to this under - studied yet important cereal crop. In constructing models for monitoring crop conditions, the number of bands used for modeling is a crucial factor affecting model accuracy. There is still no consensus on how to select appropriate wavelength variables for model construction. Moreover, the collection of spectral data is often influenced by factors such as temperature, atmospheric water vapor content, and soil background, making the elimination or reduction of spectral noise essential for building robust models (Yan et al., 2023). Numerous studies have shown that preprocessing raw spectral

http://www.aloki.hu ● ISSN 1589 1623 (Print) ● ISSN1785 0037 (Online)
DOI: http://dx.doi.org/10.15666/aeer/2302_37573771

data can effectively remove the effects of spectral noise and enhance the accuracy of monitoring models (Yang et al., 2020; Feng et al., 2022; Zheng et al., 2023), SNV minimizes scattering effects by normalizing each spectrum to zero mean and unit variance. MSC corrects additive and multiplicative scattering via linear regression against a reference spectrum. 1ST (first derivative) enhances spectral features by reducing baseline shifts and isolating absorption peaks. These methods were selected to address noise from soil background and atmospheric interference. Thus, based on these issues, this study applied several classical methods to preprocess the original spectral reflectance of foxtail millet, comparing the capabilities of full spectrum, characteristic wavelength, and optimized spectral index methods for monitoring foxtail millet AGB. This study addresses the critical gap in hyperspectral monitoring of foxtail millet AGB. We aim to (1) evaluate preprocessing methods (SNV, MSC, 1ST) for enhancing spectral correlations, (2) identify optimal spectral indices and wavelengths, and (3) develop accurate AGB estimation models to support non-destructive crop management.

Materials and methods

Experimental design

The experiment was conducted in 2023 at the Dingxiang base in Xinzhou, Shanxi Province, China. The field trials used the variety Jingu 21, with six sowing dates (B1: May 5, B2: May 12, B3: May 19, B4: May 26, B5: June 2, and B6: June 9). The planting density was 300,000 plants per hectare, with a row spacing of 30 cm, and the plot size was 5 × 6 m^2. Each trial included three replications, totaling 18 plots. Before planting, 22,500 kg/hm^2 of organic fertilizer and 375 kg/hm^2 of compound fertilizer (N:P:K = 24:10:6) were applied.

Data collection

Hyperspectral data acquisition

Hyperspectral data were collected using the FieldSpec4 portable spectroradiometer produced by Analytical Spectral Devices (ASD), USA. The spectral range spanned from 350 to 2500 nm, with a field of view of 25°. The spectral sampling intervals were 1.4 nm from 350 to 1000 nm with a spectral resolution of 3 nm, and 2 nm from 1000 to 2500 nm with a spectral resolution of 10 nm. Spectral measurements of the foxtail millet canopy were conducted from 10:00 to 14:00 under clear, calm or light wind conditions. Measurements began on July 11 (the elongation stage of the sixth sowing period) and were taken every 10 days, totaling four sessions. During measurements, the sensor probe was oriented vertically downwards at a distance of approximately 1.0 m above the canopy. Three points were measured per plot, with each point measured five times to calculate the average spectral reflectance. Standard whiteboard calibration was performed before and after each group of observations.

Biomass measurement

Following the collection of hyperspectral data, three representative foxtail millet plants were harvested from each experimental plot, quickly brought back to the laboratory, and their fresh weight was measured. The samples were then blanched at 105°C for 30 minutes and subsequently dried at 80°C until a constant weight (W/g) was achieved. The formula for calculation is as follows:

$$\mathrm{AGB} = \frac{\mathrm{W}*\mathrm{N}}{3*\mathrm{S}*100}\,(\mathrm{t/hm^2}) \quad \text{(Eq.1)}$$

http://www.aloki.hu ● ISSN 1589 1623 (Print) ● ISSN1785 0037 (Online)
DOI: http://dx.doi.org/10.15666/aeer/2302_37573771

In the formula, W represents the dry weight of three foxtail millet plants, N is the number of foxtail millet plants per plot, and S refers to the area of each experimental plot.

Construction of spectral indices

Spectral indices are calculated from remote sensing data by combining and comparing spectral characteristics across different wavelength ranges. These indices can characterize surface cover types, crop growth, and soil properties and are widely used in research and monitoring in agriculture, ecology, and water resource fields. To identify the optimal spectral indices for monitoring foxtail millet AGB, nine spectral indices were evaluated and optimized. *Table 1* lists the spectral indices used in this study along with their calculation formulas.

Table 1. *Spectral indices used in this study*

Spectral Indices	Formula	Spectral Indices	Formula
RSI	λ1/λ2	TB3	λ1/(λ2*λ3)
NDSI	(λ1-λ2)/(λ1+λ2)	TB4	λ1/(λ2+λ3)
DSI	λ1-λ2	TB5	(λ1-λ2)/ (λ1+λ2-2λ3)
TB1	(λ1-λ2)/(λ2+λ3)	TB6	(λ1-λ2+2λ3)/(λ1+λ2-2λ3)
TB2	(λ1-1.8λ2)/(λ3-1.8λ2)		

Note: λ1, λ2, and λ3 represent random wavelengths of the spectrum. (This table shows the spectral indices used in this study and their calculation formulas. Spectral indices are calculated by combining and comparing spectral characteristics across different wavelength ranges, which are used to characterize surface cover types, crop growth conditions, soil properties)

Data analysis methods

Spectral data outliers were removed using ViewSpecPro software. The Unscrambler X 10.4 was utilized for preprocessing the spectral data, which included Standard Normal Variate Transformation (SNV), Multiple Scatter Correction (MSC), and First Derivative (1ST). Correlation analysis and model construction were performed using Matlab2019, while plotting was done with Origin2021. This study evaluated model accuracy using the coefficient of determination (R^2), Root Mean Square Error (RMSE), and the Ratio of Performance to Deviation (RPD). A higher R^2, closer to 1, and a smaller RMSE indicate better model fit and predictive ability. A higher RPD value signifies better predictive capability of the model. Generally, an RPD value less than 1.4 indicates poor predictive ability; an RPD between 1.4 and 2.0 suggests good predictive capability, and an RPD of 2.0 or higher indicates excellent predictive capability (Guo et al., 2014). The calculation formula is as follows:

$$R^2 = \frac{\sum_{i=1}^{n}(Y_i{'}-\bar{Y_i})^2}{\sum_{i=1}^{n}(Y_i-\bar{Y_i})^2} \quad \text{(Eq.2)}$$

$$RMSE = \sqrt{\frac{1}{n}\sum_{i=1}^{n}(Y_i - Y_i')^2} \quad \text{(Eq.3)}$$

$$RPD = \frac{SD}{RMSE} \quad \text{(Eq.4)}$$

http://www.aloki.hu ● ISSN 1589 1623 (Print) ● ISSN1785 0037 (Online)
DOI: http://dx.doi.org/10.15666/aeer/2302_37573771

In the formula, n represents the number of samples, Y_i' and Y_i are the predicted and actual values of the samples respectively, $\bar{Y_i}$ is the mean of the actual sample values, and SD is the standard deviation of the samples.

Results

Descriptive statistical analysis of foxtail millet biomass data

As shown in *Table 2*, the dataset was divided into calibration (75%) and validation (25%) sets using a concentration gradient method to ensure representative distribution of AGB values across both subsets. From *Table 2*, it is observed that the range of foxtail millet AGB values spanned from 0.211 to 15.248 t/hm^2. Moreover, the mean values and standard deviations of the calibration set, validation set, and total samples were closely aligned. The mean values were 5.791 t/hm^2, 5.665 t/hm^2, and 5.760 t/hm^2 for the calibration, validation, and total samples, respectively. The standard deviations were 3.647 t/hm^2, 3.618 t/hm^2, and 3.614 t/hm^2 for the calibration, validation, and total samples, respectively.

Table 2. *Descriptive statistics of foxtail millet AGB*

Data set	Samples	Range	Min	Max	Mean	SD
Calibration set	54	15.037	0.211	15.248	5.791	3.647
Validation set	18	13.362	0.428	13.790	5.665	3.618
Total	72	15.037	0.211	15.248	5.760	3.614

Note: The range, minimum value, maximum value, mean, and standard deviation are t/hm^2. (The table presents the descriptive statistical results of foxtail millet AGB data. The study used the concentration gradient method to divide the data into a calibration set and a validation set at a ratio of 3:1. The table shows the number of samples, the range, minimum value, maximum value, mean value, and standard deviation of different data sets (calibration set, validation set, and total samples). These statistical information helps to understand the distribution characteristics of foxtail millet AGB data and provides basic data reference for subsequent model construction and evaluation.)

Hyperspectral response of foxtail millet biomass

To elucidate the hyperspectral response characteristics of foxtail millet biomass, this study analyzed the trends in hyperspectral changes across different gradient ranges. As shown in *Figure 1*, with the increase in foxtail millet AGB, a gradual decrease in spectral reflectance was observed within the visible and near-infrared wavelength ranges. However, within the visible light spectrum, the spectral differences between the gradient ranges of 8.000 to 12.000 t/hm^2 and 12.000 to 16.000 t/hm^2 were minimal, with noticeable changes in spectral reflectance only near the 550 nm peak.

Correlation analysis between foxtail millet biomass and canopy spectral reflectance under different preprocessing conditions

To fully extract spectral information from foxtail millet, this study applied three preprocessing methods to the raw spectral reflectance. Based on the reflectance after different preprocessings, the study analyzed the correlation between spectral reflectance and foxtail millet AGB using correlation analysis methods. As shown in *Figure 2*, the original spectral reflectance exhibited a negative correlation with foxtail millet biomass

http://www.aloki.hu ● ISSN 1589 1623 (Print) ● ISSN1785 0037 (Online)
DOI: http://dx.doi.org/10.15666/aeer/2302_37573771

across the entire spectral range, with the maximum absolute correlation coefficient (MACC) being 0.612. After preprocessing with SNV, MSC, and 1ST, the correlation between spectral reflectance and foxtail millet biomass showed fluctuating positive and negative correlations across the full spectrum. The correlation trends for MSC and SNV were similar, while 1ST showed greater fluctuations. From the right graph, it is evident that all three preprocessing methods enhanced the correlation between foxtail millet AGB and spectral reflectance. Notably, the correlation after MSC preprocessing was significantly improved, with the MACC value reaching 0.784.

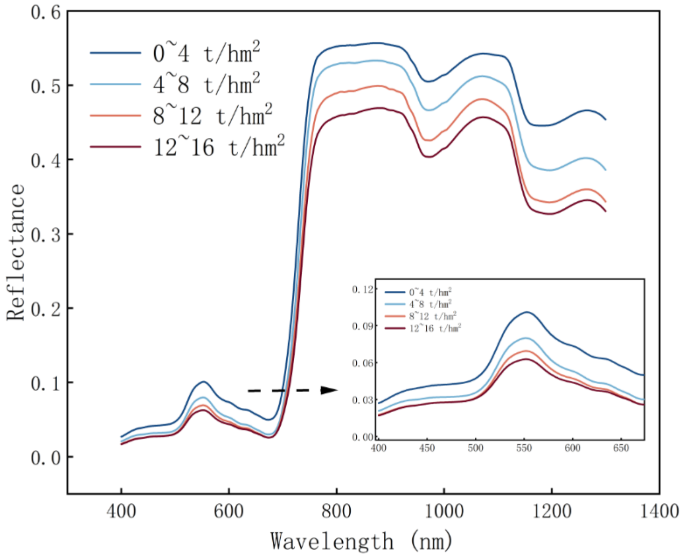

Figure 1. *Hyperspectral characteristics of AGB of foxtail millet in different gradient ranges. (The figure shows the hyperspectral characteristics of foxtail millet under different AGB gradient ranges. The abscissa represents the wavelength (nm), and the ordinate represents the spectral reflectance. The curves of different colors represent the AGB gradient ranges of 0 ~ 4 t/hm², 4 ~ 8 t/hm², 8 ~ 12 t/hm², and 12 ~ 16 t/hm²)*

Extraction of characteristic wavelengths for foxtail millet biomass

To explore the characteristic wavelengths of foxtail millet biomass and reduce the redundancy in the original spectral data, this study utilized the Successive Projection Algorithm (SPA) to extract ten characteristic wavelengths from the foxtail millet biomass following preprocessing of the original spectral reflectance. As shown in *Table 3*, preprocessing significantly altered the characteristic wavelengths of the foxtail millet. The characteristic wavelengths of the original spectral reflectance were distributed between 409 nm and 1300 nm. After SNV preprocessing, the characteristic wavelengths ranged between 516 nm and 751 nm, and 958 nm to 1140 nm. Following MSC preprocessing, they ranged between 574 nm and 761 nm, and 956 nm to 1141 nm. After 1ST preprocessing, the wavelengths were distributed between 447 nm and 1073 nm. This indicates that different preprocessing methods affect the extraction of information from spectral data differently.

http://www.aloki.hu ● ISSN 1589 1623 (Print) ● ISSN1785 0037 (Online)
DOI: http://dx.doi.org/10.15666/aeer/2302_37573771

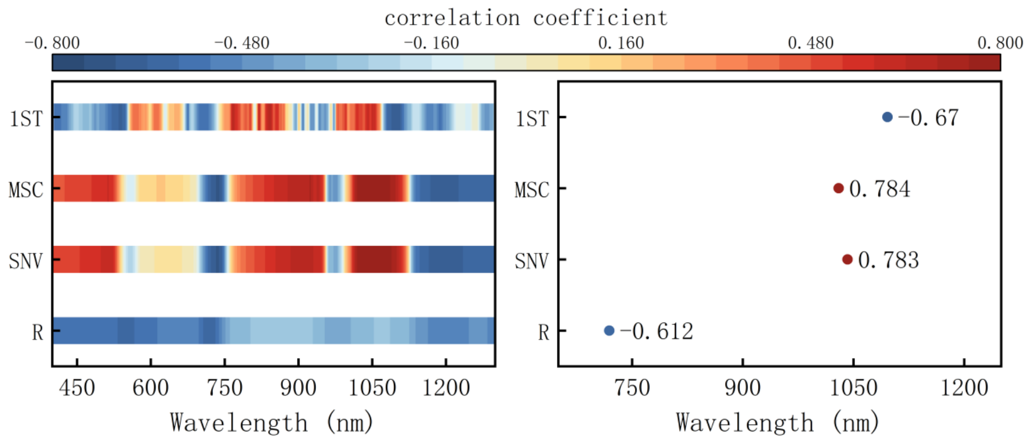

***Figure 2.** Correlation analysis of spectral reflectance with foxtail millet AGB after preprocessing. (The figure presents the correlation analysis results between the spectral reflectance after preprocessing and the AGB of foxtail millet. The abscissa is the wavelength (nm), and the ordinate is the correlation coefficient. The curves of different colors represent the correlations between the spectral reflectances after original spectral reflectance (R), Standard Normal Variate (SNV), Multiplicative Scatter Correction (MSC), and First Derivative (1ST) preprocessing and AGB)*

***Table 3.** Characteristic wavelength of foxtail millet*

Preprocessing method	Characteristic wavelength (nm)
R	746/904/459/675/719/1146/554/1300/409/934
SNV	516/751/589/1001/1140/1108/958/1124/547/678
MSC	1141/761/1110/1028/956/740/1126/574/994/673
1ST	999/525/1003/831/447/900/1073/671/976/968

Note: Original Spectral Reflectance(R), Standard Normal Variate (SNV), Multiple Scattering Correction (MSC), First Derivative (1ST)

Selection of optimal spectral indices

As shown in *Figures 3 and 4*, based on the preprocessing of the original spectral reflectance, this study employed an exhaustive method to calculate the correlation between all possible combinations of spectral indices and foxtail millet AGB. *Table 4* lists the selected optimal spectral indices. From *Table 4*, it can be seen that among the dual-band spectral indices, the R-RSI (766, 762) constructed from the original spectral reflectance has a correlation coefficient with foxtail millet AGB of 0.788. The spectral indices SNV-RSI (572, 1045) and MSC-NDSI (765, 766), constructed from SNV and MSC preprocessed reflectance respectively, achieved correlation coefficients of 0.803 and 0.794 with foxtail millet AGB. The 1ST-DSI (537, 684), constructed from 1ST preprocessed reflectance, reached a correlation coefficient of 0.824 with foxtail millet AGB.

In the category of three-band spectral indices, the R-TB5 (703, 430, 513) constructed from the original spectral reflectance had a correlation coefficient of 0.830 with foxtail millet AGB. The R-TB5 (450, 696, 449) constructed from SNV preprocessed reflectance achieved a correlation coefficient of 0.837, and the MSC-TB6 (720, 400, 528) constructed from MSC preprocessed reflectance reached a correlation coefficient of 0.839. The 1ST-

http://www.aloki.hu ● ISSN 1589 1623 (Print) ● ISSN1785 0037 (Online)
DOI: http://dx.doi.org/10.15666/aeer/2302_37573771

TB1 (450, 625, 536), constructed from 1ST preprocessed reflectance, showed the highest correlation with foxtail millet AGB, achieving a correlation coefficient of 0.863. It is evident that the 1ST preprocessing method significantly enhanced the effective information from the spectra, improving the correlation between the spectral indices and foxtail millet AGB. Furthermore, the three-band spectral indices showed superior correlation with foxtail millet AGB compared to the dual-band spectral indices, and correlation coefficients >0.8 indicate strong predictive potential for AGB, enabling farmers to adjust irrigation and fertilization in real time.

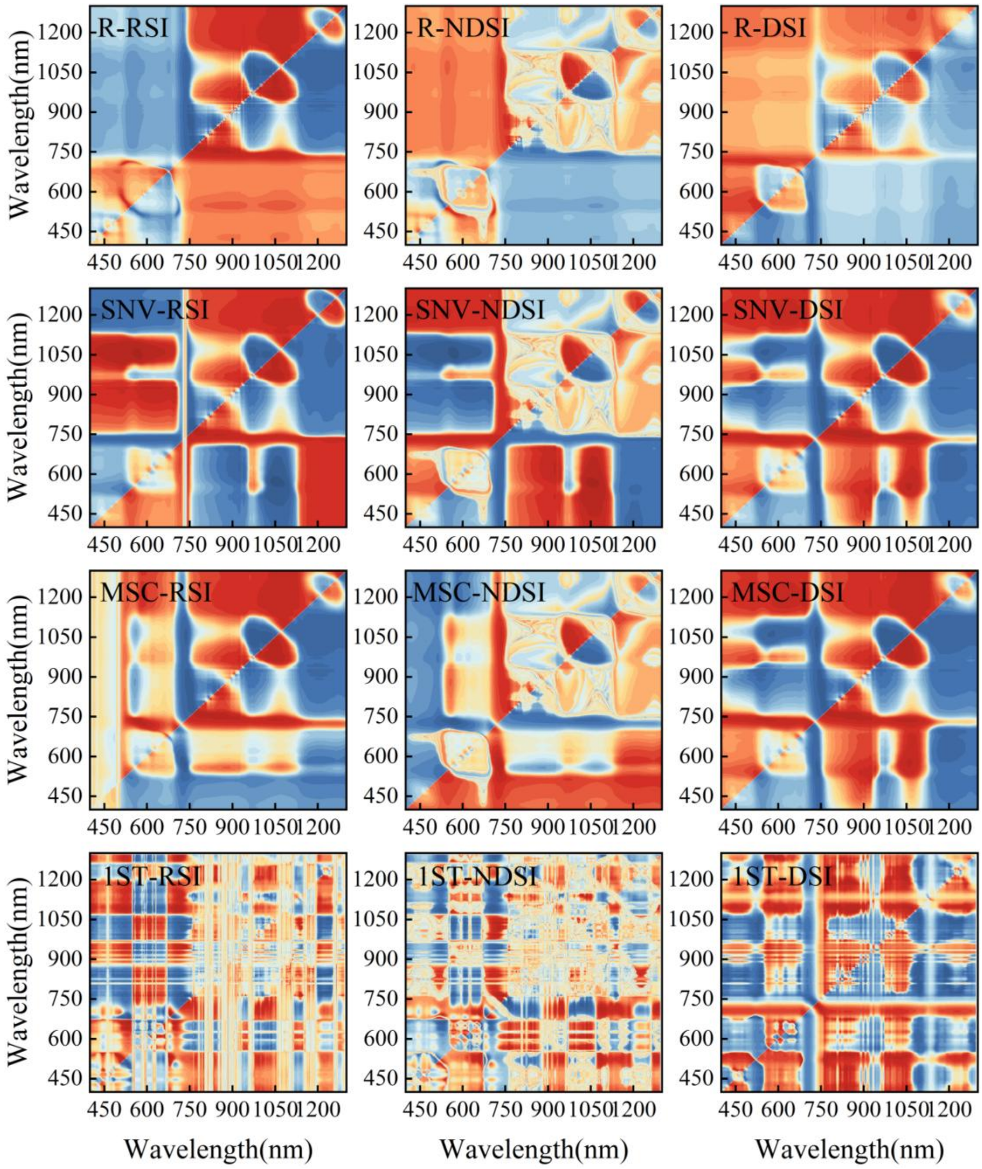

Figure 3. *Correlation coefficient plots between dual-band spectral indices and AGB of foxtail millet. (The figure shows the correlation coefficient plots between dual - band spectral indices and the AGB of foxtail millet. The abscissa is the wavelength (nm), and the ordinate is the correlation coefficient. The curves of different colors represent the correlations between different dual - band spectral indices (RSI, NDSI, DSI,) constructed from the original spectral reflectance (R), SNV - preprocessed reflectance, MSC - preprocessed reflectance, and 1ST - preprocessed reflectance and AGB)*

http://www.aloki.hu ● ISSN 1589 1623 (Print) ● ISSN1785 0037 (Online)
DOI: http://dx.doi.org/10.15666/aeer/2302_37573771

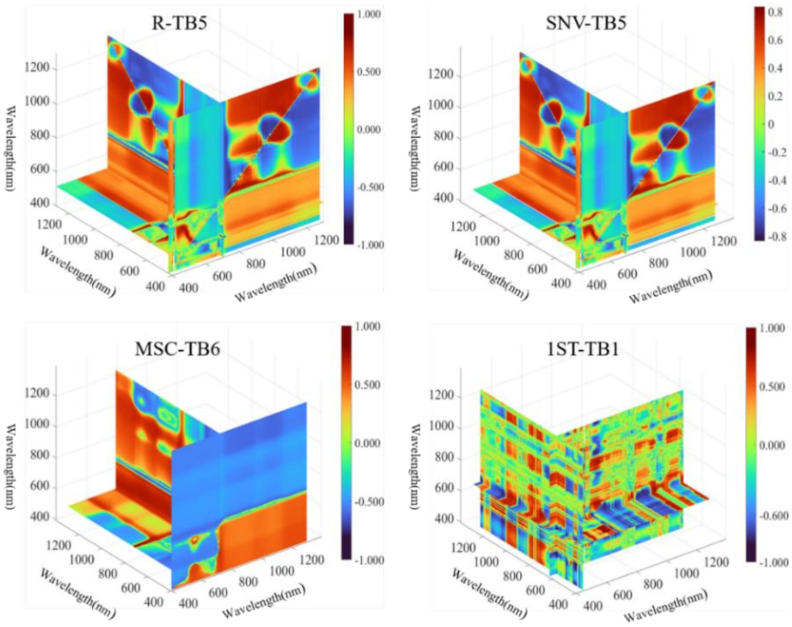

Figure 4. *Correlation coefficient plot between three-band spectral index and AGB of foxtail millet. (The figure presents the correlation coefficient plot between three - band spectral indices and the AGB of foxtail millet. The abscissa is the wavelength (nm), and the ordinate is the correlation coefficient. The curves of different colors represent the correlations between different three - band spectral indices (TB1, TB5, TB6) constructed from the original spectral reflectance (R), SNV - preprocessed reflectance, MSC - preprocessed reflectance, and 1ST - preprocessed reflectance and AGB)*

Table 4. *Optimal spectral bands and correlation coefficients*

	R	SNV	MSC	1ST
RSI	(766, 762) 0.788	(572, 1045) 0.803	(767, 765) 0.790	(686, 542) 0.803
NDSI	(766, 765) 0.786	(765, 767) 0.802	(765, 766) 0.794	(849, 1209) 0.805
DSI	(846, 848) 0.748	(765, 767) 0.786	(765, 767) 0.785	(537, 684) 0.824
TB1	(764, 760, 759) 0.801	(401, 1019, 514) 0.809	(522, 815, 614) 0.812	(451, 626, 697) 0.863
TB2	(770, 549, 761) 0.810	(1020, 459, 432) 0.824	(741, 515, 400) 0.826	(486, 510, 495) 0.856
TB3	(504, 736, 676) 0.792	(1013, 596, 514) 0.816	(882, 1114, 760) 0.815	(846, 1230, 1209) 0.831
TB4	(983, 1271, 762) 0.816	(400, 1020, 516) 0.821	(998, 1260, 759) 0.817	(680, 904, 691) 0.840
TB5	(703, 430, 513) 0.830	(710, 434, 520) 0.837	(703, 432, 515) 0.835	(904, 680, 696) 0.849
TB6	(719, 675, 512) 0.820	(1031, 400, 513) 0.829	(720, 400, 528) 0.839	(511, 464,505) 0.837

Note: The table shows the optimal spectral bands constructed based on different preprocessed spectral reflectances and their correlation coefficients with the AGB of foxtail millet. The study calculated the correlations between all possible combinations of spectral indices and the AGB of foxtail millet to screen out the optimal spectral bands. It can be seen from the table that among the dual - band spectral indices

Evaluation of the accuracy of foxtail millet AGB monitoring models

This study constructed three types of foxtail millet AGB monitoring models based on the full spectrum, characteristic wavelengths, and optimized spectral indices. *Table 5* displays the performance of the foxtail millet AGB monitoring models. It is evident that the models constructed using spectral data preprocessed with 1ST were the best among

http://www.aloki.hu ● ISSN 1589 1623 (Print) ● ISSN1785 0037 (Online)
DOI: http://dx.doi.org/10.15666/aeer/2302_37573771

the three types (*Table 5*). Among these, the best performing foxtail millet AGB monitoring model was the 1ST-PLS model based on the full spectrum, which achieved an R^2 of 0.834, RMSE of 1.443 t/hm^2, and RPD of 2.507. This was followed by the 1ST-TB1 model based on optimized spectral indices, with an R^2 of 0.823, RMSE of 1.516 t/hm^2, and RPD of 2.387, and lastly the 1ST-SPA-PLS model based on characteristic wavelengths, which had an R^2 of 0.790, RMSE of 1.721 t/hm^2, and RPD of 2.100. Therefore, it can be seen that the 1ST spectral preprocessing method significantly enhances model accuracy. *Figure 5* shows the fitting plots of the best models among the three types, indicating that all three models achieved good fitting results and can accurately monitor foxtail millet AGB.

Table 5. *Evaluation of the accuracy of the foxtail millet AGB monitoring models*

models	R^2	RMSE	RPD
R-PLS	0.726	1.867	1.936
SNV-PLS	0.805	1.639	2.205
MSC-PLS	0.793	1.688	2.141
1ST-PLS	0.834	1.443	2.507
R-SPA-PLS	0.664	2.137	1.691
SNV-SPA-PLS	0.686	1.996	1.811
MSC-SPA-PLS	0.699	1.948	1.856
1ST-SPA-PLS	0.790	1.721	2.100
1ST-TB1	0.823	1.516	2.387

Note: The table evaluates the accuracy of the foxtail millet AGB monitoring models constructed based on the full spectrum, characteristic wavelengths, and optimized spectral indices. Three indicators, the coefficient of determination (R^2), Root Mean Square Error (RMSE), and Ratio of Performance to Deviation (RPD), are used to measure the model performance. Generally, the closer R^2 is to 1 and the smaller RMSE is, the better the fitting and predictive ability of the model; the higher the RPD value, the stronger the predictive ability of the model

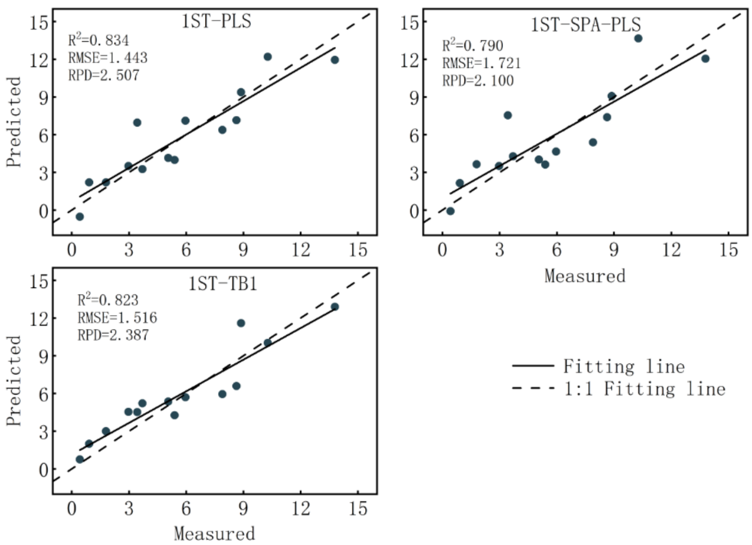

Figure 5. *Fitting plots of AGB optimal model for foxtail millet. (The figure shows the fitting plots of the AGB optimal models for foxtail millet. The abscissa represents the measured values, and the ordinate represents the predicted values. The curves of different colors represent the fitting situations of the 1ST - PLS model based on the full spectrum, the 1ST - SPA - PLS model based on characteristic wavelengths, and the 1ST - TB1 model based on optimized spectral indices)*

http://www.aloki.hu ● ISSN 1589 1623 (Print) ● ISSN1785 0037 (Online)
DOI: http://dx.doi.org/10.15666/aeer/2302_37573771

Discussion

In crop - related research, the accuracy of research results is highly dependent on the pre - treatment methods. The methods used in this study, such as SNV, MSC, and 1ST, have been widely applied and validated in relevant fields. Rinnan et al. (2009) indicated that MSC and SNV can effectively enhance the signal - to - noise ratio of spectral data and eliminate the interference of the medium on the spectral curve during the light propagation process. Yang et al. (2022) and Yan et al. (2023) compared multiple pretreatment methods and concluded that the model constructed after 1ST pretreatment had a relatively high accuracy, which is consistent with the conclusion of this study.

This study, based on preprocessing the original spectral reflectance of foxtail millet AGB, explored the capabilities of optimized spectral indices, characteristic wavelength methods, and full-spectrum methods in monitoring foxtail millet AGB. The study found that besides the spectral reflectance after 1ST preprocessing, the best spectral indices from combinations of dual-band optimized using raw, SNV, and MSC preprocessed spectral reflectances were all around 760 nm. Similarly, characteristic wavelengths selected using SPA also included wavelengths around 760 nm. Previous research, such as that by Cao et al. (2022), which studied the optimal vegetation index and appropriate bandwidth for monitoring the above-ground biomass of peanuts, showed that the Normalized Red Edge Index (NDRE) (λ790, λ720) had high monitoring accuracy. Hansen et al. (2003) used the Normalized Difference Vegetation Index (NDVI) and Partial Least Squares (PLS) for estimating the above-ground biomass of wheat, found that NDVI had a high correlation with biomass in the central wavelength range of 680–750 nm.

Among the dual-band spectral indices, the 1ST-DSI (537, 684) showed the highest correlation with foxtail millet AGB, with a correlation coefficient of 0.824, Wang et al. (2024) pointed out the vegetation index DVI has the highest correlation with the biomass throughout the entire growth period of rice, which is consistent with the conclusion of this study. In the three-band spectral indices, the 1ST-TB1 (451, 626, 697) had the highest correlation with foxtail millet AGB, with a correlation coefficient of 0.863, the optimized three-band algorithm is an attractive tool for optimizing and identifying central bands (Li et al., 2021a). The three-band spectral indices showed significantly higher correlation with foxtail millet AGB compared to the dual-band indices, indicating that three-band indices can more fully utilize spectral information and mitigate the saturation issues of dual-band indices (Zhang et al., 2022). The accuracy of the three types of foxtail millet AGB monitoring models built showed that models based on 1ST-preprocessed spectral reflectance had significantly improved accuracy compared to those based on raw spectral reflectance. This improvement could be due to the reduction or elimination of spectral noise affecting the spectral reflectance of the foxtail millet canopy, achieved through 1ST preprocessing. Previous studies in crop growth spectral monitoring also demonstrated that 1ST is an effective method to eliminate spectral noise (Gao et al., 2020; Tong et al., 2022). This study further confirms that 1ST is an effective method for processing hyperspectral data, contributing significantly to the improved accuracy of foxtail millet AGB monitoring models.

Moreover, this research determined that the optimal model for monitoring foxtail millet AGB was the 1ST-PLS (R^2=0.834; RMSE=1.443 t/hm^2; RPD=2.507), which has high accuracy in monitoring plant biomass (Liu et al., 2021, 2022; ElHendawy et al., 2022). However, the 1ST-TB1 model built using optimized spectral indices also showed high accuracy (R^2=0.823; RMSE=1.516 t/hm^2; RPD=2.387). Compared to the 1ST-PLS monitoring model, although the accuracy of the 1ST-TB1 model was slightly lower, the

http://www.aloki.hu ● ISSN 1589 1623 (Print) ● ISSN1785 0037 (Online)
DOI: http://dx.doi.org/10.15666/aeer/2302_37573771

full spectrum model is more complex, using up to 900 wavelengths, while the 1ST-TB1 model used only three wavelengths. Therefore, considering the complexity of the models, the 1ST-TB1 model demonstrates an outstanding phenotype. The 1ST-TB1 index and 1ST-PLS model highlight the potential of hyperspectral technology to mitigate spectral saturation and environmental noise, offering scalable solutions for diverse crops. Their integration into UAV or satellite-based systems could revolutionize large-scale biomass monitoring, particularly in resource-limited regions where foxtail millet is a staple crop. In this study, the foxtail millet AGB monitoring model built using the characteristic wavelength method achieved the highest R^2 of 0.790. In contrast, the model built using the full spectrum achieved the highest R^2 of 0.852, indicating that the characteristic wavelengths selected by SPA did not contain all effective information of foxtail millet AGB. Considering that too many wavelengths might also lead to redundancy and increased complexity of the models, developing hyperspectral models for agriculture, future research should balance wavelength selection to avoid redundancy and simplify models for field deployment. Next, integrate UAV - based systems and validate across diverse zones. Also, incorporate multi - temporal data and machine learning to mitigate environmental impacts for more accurate models, in previous research on constructing crop biomass monitoring models, different models have demonstrated diverse advantages. Some studies have indicated that the Random Forest (RF) (Xian et al., 2024; Dong et al., 2024b) model performs optimally, while others have pointed out that the Convolutional Neural Network (CNN) (Zhou et al., 2024) exhibits higher accuracy. Based on this, to effectively improve the monitoring accuracy of foxtail millet biomass, it is necessary to comprehensively apply multiple machine learning methods.

This technology can accurately acquire real - time information on the growth of foxtail millet, enabling the fine - grained management of water and fertilizer resources. It effectively prevents resource waste and environmental pollution, thereby enhancing the resilience of the agricultural system in the face of climate change and providing strong support for the development of global sustainable agriculture.

Conclusion

The 1ST-PLS model built on the full spectrum could accurately monitor foxtail millet AGB (R^2=0.834; RMSE=1.443 t/hm^2; RPD=2.507). This achievement can contribute to precision agriculture, enabling accurate understanding of foxtail millet growth conditions. It provides a scientific basis for rational resource allocation and determination of harvest time, thus enhancing agricultural production efficiency.

Acknowledgements. This work was supported by the hyperspectral monitoring study of photoperiod sensitivity traits in foxtail millet (CXGC2023038), precise identification of foxtail millet germplasm resources in the summer millet region (19240649), and funding for the "Technology Innovation Enhancement Project" by Shanxi Agricultural University.

REFERENCES

[1] Cao, Z. S., Li, Y. D., Huang, J. B., Sun, B. F., Ye, C., Shu, S. F., Wu, L. F., Tian, Y. C. (2022): Sensitive vegetation indices and optimal bandwidths for monitoring peanut LAI and AGB. – Chinese Journal of Oil Crop Sciences 44(6): 1320-1328.

[2] Diao, X. M. (2019): Progresses in stress tolerance and field cultivation studies of orphan cereals in China. – Scientia Agricultura Sinica 52(22): 3943-3949.
[3] Dong, Z., Yang, W. D., Zhang, M. J., Zhu, H. F., Wang, C. (2019): Estimation models of maize leaf SPAD value based on hyperspectral remote sensing. – Crops 3: 126-131.
[4] Dong, E. W., Wang, Y., Wang, J. S., Liu, Q. X., Huang, X. L., Jiao, X. Y. (2024a): Effects of nitrogen fertilization levels on grain yield, plant nitrogen utilization characteristics and grain quality of foxtail millet. – Scientia Agricultura Sinica 57(2): 306-318.
[5] Dong, Z. Y., Lv, S. Q., Wei, Y. X., Zhu, Y. W., Meng, X. X. (2024b): Estimation of Aboveground Biomass of Rape Based on UAV - borne Multispectral Remote Sensing. – South China Agriculture 18(13): 172-177.
[6] ElHendawy, S., AlSuhaibani, N., Mubushar, M., Tahir, M. U., Marey, S., Refay, Y., Tola, E. (2022): Combining hyperspectral reflectance and multivariate regression models to estimate plant biomass of advanced spring wheat lines in diverse phenological stages under salinity conditions. – Applied Sciences 12(4): 1983.
[7] Feng, Z. H., Li, X., Duan, J. Z., Gao, F., He, L., Yang, T. C., Rong, Y. S., Song, L., Yin, F. (2022): Hyperspectral remote sensing monitoring of wheat powdery mildew based on feature band selection and machine learning. – Acta Agronomica Sinica 48(9): 2300-2314.
[8] Gao, Y., Wang, Y. C., Gu, X. H., Zhou, X. W., Ma, Y., Xuan, X. Y. (2020): Quantitative inversion of soil organic matter and total nitrogen content based on differential transformation. – Jiangsu Agricultural Sciences 48(24): 220-225.
[9] Gong, R. X., Lu, X. H., Zhang, H. N., Wang, Q., Chen, Z. Q., Yang, B. C., Ma, L. L. (2023): Model analysis of estimating soybean above-ground biomass by hyperspectral vegetation index. – Soybean Science 42(3): 352-359.
[10] Guo, D. D., Huang, S. M., Zhang, S. Q., Nie, S. W. (2014): Comparative analysis of various hyperspectral prediction models of fluvo-aquic soil organic matter. – Transactions of the Chinese Society of Agricultural Engineering 30(21): 192-200.
[11] Hansen, P. M., Schjoerring, J. K. (2003): Reflectance measurement of canopy biomass and nitrogen status in wheat crops using normalized difference vegetation indices and partial least squares regression. – Remote Sensing of Environment 86(4): 542-553.
[12] Jiang, Y., Wang, L., Yang, Y., Cai, Y. T., Zhang, X. H., Wang, H. Z., Wang, S. D. (2022): Application of UAV hyperspectral imaging technology in crop growth information monitoring. – Journal of Northeast Agricultural University 53(3): 88-96.
[13] Kang, L., Gao, R., Kong, Q. M., Jia, Y. J., Shi, Y. B., Su, Z. B. (2020): Estimation of SPAD value of rice leaves based on hyperspectral image. – Journal of Northeast Agricultural University 51(10): 89-96.
[14] Kuplich, T. M., Curran, P. J., Atkinson, P. M. (2005): Relating SAR image texture to the biomass of regenerating tropical forests. – International Journal of Remote Sensing 26(21): 4829-4854.
[15] Lata, C., Gupta, S., Prasad, M. (2013): Foxtail millet: A model crop for genetic and genomic studies in bioenergy grasses. – Critical Reviews in Biotechnology 33(3): 328-343.
[16] Li, F., Li, D., Elsayed, S., Hu, Y. C., Schmidhalter, U. (2021a): Using optimized three-band spectral indices to assess canopy N uptake in corn and wheat. – European Journal of Agronomy 127: 126286.
[17] Li, G. Y., Cong, X. J., Li, G. Q. (2021b): Effects of sowing date on agronomic characters, yield and quality of foxtail millet variety Jinxuan 6. – Shandong Agricultural Sciences 53(3): 36-40.
[18] Li, S. G., Liu, F., Liu, M., Cheng, R. H., Xia, E. J., Diao, X. M. (2021c): Current status and future prospective of foxtail millet production and seed industry in China. – Scientia Agricultura Sinica 54(3): 459-470.
[19] Li, G. Y., Cong, X. J., Li, G. Q., Zhao, N., Chen, E. Y., Li, L. (2022a): Effect of sowing date of foxtail millet on crop productivity in foxtail millet/peanut intercropping system. – Journal of Nuclear Agricultural Sciences 36(5): 1008-1016.

http://www.aloki.hu ● ISSN 1589 1623 (Print) ● ISSN1785 0037 (Online)
DOI: http://dx.doi.org/10.15666/aeer/2302_37573771

[20] Li, S. G., Liu, F., Liu, M., Zhao, W. Q., Zhao, Y. (2022b): Historical evolution and future development direction of foxtail millet planting in China. – Science and Technology of Cereals, Oils and Foods 30(4): 60-67+10.

[21] Liu, Y., Zhang, H., Feng, H. K., Sun, Q., Huang, J., Wang, J. J., Yang, G. J. (2021): Estimation of potato above ground biomass based on hyperspectral images of UAV. – Spectroscopy and Spectral Analysis 41(9): 2657-2664.

[22] Liu, Y., Feng, H. K., Yue, J. B., Li, Z. H., Jin, X. L., Fan, Y. G., Feng, Z. H., Yang, G. J. (2022): Estimation of aboveground biomass of potatoes based on characteristic variables extracted from UAV hyperspectral imagery. – Remote Sensing 14(20): 5121.

[23] Lv, J. Z. (2020): Advance in genetic diversity analysis of foxtail millet. – Journal of Hebei Agricultural University 43(5): 40-45.

[24] Marshall, M., Thenkabail, P. (2015): Developing in situ non-destructive estimates of crop biomass to address issues of scale in remote sensing. – Remote Sensing 7(1): 808-835.

[25] Rinnan, A., van den Berg, F., Engelsen, S. B. (2009): Review of the most common pre-processing techniques for near-infrared spectra. – Trends in Analytical Chemistry 28(10): 1201-1222.

[26] Tong, X., Yang, Z. L., Zhang, Y. R., Wu, Y. C., Duan, L. M. (2022): Estimation of pasture aboveground biomass using different orders of differential hyperspectral vegetation indices. – Acta Agrestia Sinica 30(9): 2438-2448.

[27] Wang, W. K., Zhang, J. Y., Wang, H., Cao, Q., Tian, Y. C., Zhu, Y., Cao, W. X., Liu, X. J. (2023a): Non-destructive monitoring of rice growth key indicators based on fixed-wing UAV multispectral images. – Scientia Agricultura Sinica 56(21): 4175-4191.

[28] Wang, X. F., Liang, D. L., Li, Z. Y., Chen, Y. J., Jiang, J. F., Zheng, A. H., Gao, T. T., Ren, X. L. (2023b): Response of dry matter distribution and transport in millet covered with plastic film to planting density. – Molecular Plant Breeding 21(23): 7959-7966.

[29] Wang, D., Sun, R., Su, Y., Yang, B. (2024): Rice biomass estimation based on multispectral imagery from unmanned aerial vehicles. – Transactions of the Chinese Society of Agricultural Engineering 40(17): 161-170.

[30] Xian, G. L., Liu, J. G., Lin, Y. X., Li, S., Bian, C. S. (2024): Multi-Feature Fusion for Estimating Above-Ground Biomass of Potato by UAV Remote Sensing. – Plants 13(23): 3356.

[31] Xie, Y. K., Song, J. Y., Liu, M., Meng, W. Z., Feng, M. C., Wang, C., Yang, W. D., Qiao, X. X., Yang, C. B. (2023): Hyperspectral monitoring of proline content in winter wheat under water stress. – Chinese Journal of Applied Ecology 34(2): 463-470.

[32] Yan, X. B., Wang, Z. G., Wang, Y. X., Feng, M. C., Wang, C., Xiao, L. J., Yu, J. T., Yang, W. D. (2022): Hyperspectral monitoring of effects of drought stress on photosynthetic pigment content of winter wheat. – Journal of Shanxi Agricultural Sciences 50(9): 1269-1277.

[33] Yan, X. B., Qiao, X. X., Yang, S., Feng, M. C., Song, X. Y., Zhang, M. J., Xiao, L. J., Zhang, Z., Shafiq, F., Yang, W. D., Wang, C. (2023): Hyperspectral response and monitoring study of soil moisture content based on the optimized spectral index. – Soil Science Society of America Journal 87(2): 216-230.

[34] Yang, H., Yang, G. J., Gaulton, R., Zhao, C. J., Li, Z. H., Taylor, J., Wicks, D., Minchella, A., Chen, E., Yang, X. T. (2019a): In-season biomass estimation of oilseed rape (*Brassica napus* L.) using fully polarimetric SAR imagery. – Precision Agriculture 20(3): 630-648.

[35] Yang, Y. B., Zhang, H., Wang, R. F., Deng, L. G., Qin, L., Chen, E. Y., Guan, Y. A. (2019b): Determination of yellow pigment content in foxtail millet. – Journal of the Chinese Cereals and Oils Association 34(3): 121-125.

[36] Yang, S., Wang, C., Yang, W. D., Feng, M. C., Liu, T. T., Qiao, X. X., Li, G. X., Zhang, X., Xu, J., Zhang, Y. (2020): Effect of pretreatments on spectral estimation of soil organic matter (SOM). – Journal of Shanxi Agricultural Sciences 48(10): 1637-1640+1645.

[37] Yang, C. B., Feng, M. C., Song, L. F., Jing, B. H., Xie, Y. K., Wang, C., Qin, M. X., Yang, W. D., Xiao, L. J., Sun, J. J., Zhang, M. J., Song, X. Y., Kubar, M. S. (2022): Hyperspectral

http://www.aloki.hu ● ISSN 1589 1623 (Print) ● ISSN1785 0037 (Online)
DOI: http://dx.doi.org/10.15666/aeer/2302_37573771

monitoring of soil urease activity under different water regulation. – Plant and Soil 475(1-2): 431-446.
[38] Yue, J. B., Yang, G. J., Tian, Q. J., Feng, H. K., Xu, K. J., Zhou, C. Q. (2019): Estimate of winter-wheat above-ground biomass based on UAV ultrahigh-ground-resolution image textures and vegetation indices. – ISPRS Journal of Photogrammetry and Remote Sensing 150: 226-244.
[39] Zhang, X., Sun, H., Qiao, X. X., Yan, X. B., Feng, M. C., Xiao, L. J., Song, X. Y., Zhang, M. J., Shafiq, F., Yang, W. D., Wang, C. (2022): Hyperspectral estimation of canopy chlorophyll of winter wheat by using the optimized vegetation indices. – Computers and Electronics in Agriculture 193: 106654.
[40] Zhang, M., Liu, T., Sun, C. M. (2023): Wheat biomass estimation based on UAV hyperspectral data. – Journal of Anhui Agricultural Sciences 51(17): 182-186+189.
[41] Zhao, S. L., Mujahid, H., Wang, G. B., Bian, Z. H., Wang, M., Lan, Y. B. (2024): Research progress of crop growth monitoring based on UAV remote sensing. – Jiangsu Agricultural Sciences 52(8): 8-15.
[42] Zheng, Z. K., Chang, Q. R., Jiang, S. Y., Fu, X. T., Li, K., Zhang, Z. J., Mo, H. Y. (2023): Estimation of maize SPAD value based on fractional differential of UAV hyperspectral. – Journal of Northeast Agricultural University 54(2): 66-74.
[43] Zhou, M. G., Yan, Y. C., Gao, W., He, J. Y., Li, X. S., Niu, Z. J. (2014): Estimating Aboveground Biomass of Maize Based on Multispectral Remote Sensing and Convolutional Neural Network. – Transactions of the Chinese Society for Agricultural Machinery 55(9): 238-248.
[44] Zhu, C. C., Fu, S. J., Qin, N., Wang, C. Y., Dai, S. T., Song, Y. H., Wei, X., Li, J. X. (2023a): Effects of phosphorus fertilizer application depth on root distribution, nitrogen uptake and utilization and yield of foxtail millet. – Journal of Henan Agricultural Sciences 52(12): 22-30.
[45] Zhu, Y. J., Tao, X. Y., Chen, X. F., Su, X. X., Liu, J. K., Li, X. W. (2023b): Estimation of above-ground biomass of winter wheat based on vegetation indexes and texture features of multispectral images captured by unmanned aerial vehicle. – Acta Agriculturae Zhejiangensis 35(12): 2966-2976.

http://www.aloki.hu ● ISSN 1589 1623 (Print) ● ISSN1785 0037 (Online)
DOI: http://dx.doi.org/10.15666/aeer/2302_37573771